

Electronic Supplementary Information (*ESI*)

Polar Stacking of Molecules in Liquid Chloroform

J. J. Shephard,^{a,b} A. K. Soper,^c S. K. Callear,^c S. Imberti,^c J. S. O. Evans^b and C. G. Salzmann^{a*}

^a Department of Chemistry, University College London, 20 Gordon Street, WC1H 0AJ London, UK

^b Department of Chemistry, Durham University, South Road, Durham DH1 3LE, UK

^c ISIS Facility, Rutherford Appleton Laboratory, Didcot OX11 0QX, UK

* Corresponding author: c.salzmann@ucl.ac.uk (C. G. Salzmann)

Table of Contents

1	Materials	2
2	Neutron diffraction experiments.....	2
3	Data modeling	3
4	Structural analysis	5
5	Comparison with X-ray diffraction data.....	5
6	Kirkwood correlation factor from dielectric spectroscopy and the <i>EPSR</i> -derived model.....	6
7	References	7

1 Materials

Chloroform (CHCl_3) and deuterated chloroform (CDCl_3) were purchased from Sigma Aldrich and used without further purification. The liquids, with quoted purities of 99.9 weight% and 99.96 D / H atom%, contained ~200 ppm of amylene as a chemical stabilizer to prevent the formation of phosgene.

2 Neutron diffraction experiments

$\text{Ti}_{0.68}\text{Zr}_{0.32}$ null-scattering alloy sample cells with internal dimensions of $1 \times 38 \times 38$ mm were used to contain the two neat liquids as well as a 50 mol% mixture of CHCl_3 and CDCl_3 during the neutron scattering measurements. These were carried out at 25 and -53°C for ~1000 μA h of proton current on the Small Angle Neutron Diffractometer for Amorphous and Liquid Samples (SANDALS) at the ISIS spallation neutron source at the Rutherford Appleton Laboratory, UK.

SANDALS detects neutrons scattered by a sample at angles between 3.9 and 39° , and covers a wavevector-transfer range of $0.1 - 50 \text{ \AA}^{-1}$. The wavevector transfer, Q , is calculated from the wavelengths of the incident neutrons, λ , and their scattering angles, 2θ , according to:

$$Q = \frac{4\pi}{\lambda} \sin \theta \quad \text{Eq. S1}$$

The raw data were corrected for absorption and multiple scattering using the *GudrunN* software package which was also used to subtract the perturbation to the data caused by inelastic collisions.¹ These inelasticity features were removed using the *Iterate Gudrun* routine in *GudrunN* to give the total structure factors, $F(Q)$, of the liquids. The datasets collected at 25 and -53°C are shown in Figure 1 and Figure S1, respectively.

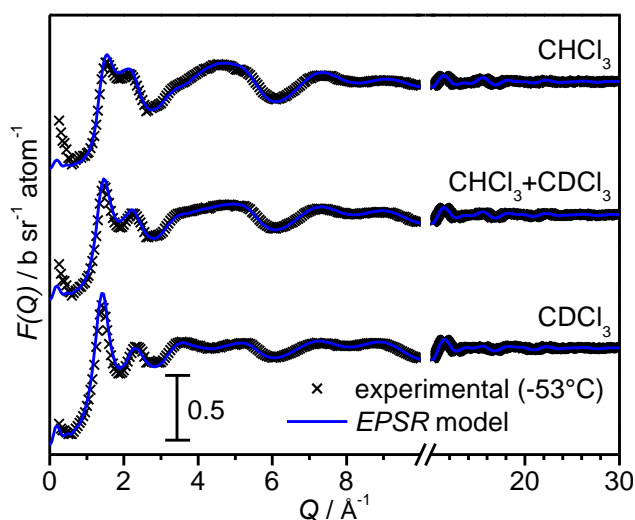


Figure S1. Experimental (black crosses) and *EPSR*-derived (blue lines) total structure factors for chloroform liquids at -53°C .

3 Data modeling

To produce suitable starting structures of liquid chloroform for modeling the experimental diffraction data a standard Monte Carlo simulation was carried out using the *EPSR* (empirical potential structure refinement) programme.^{2,3} For this, a cubic box with dimensions of 58.5298 Å (56.9057 Å) was filled with 1500 CHCl₃ molecules giving an atomic density of 0.037405 atoms Å⁻³ (0.040700 atoms Å⁻³) consistent with the experimental density at 25°C (-53°C).⁴ The average bond lengths and angles of chloroform were taken from a microwave experiment,⁵ whereas the Lennard-Jones parameters and partial charges used were determined by Barlette *et al.*⁶ (Table S1).

Table S1. Average bond lengths, r_{A-B} , and angles, γ_{A-B-C} , Lennard-Jones parameters, σ and ε , and partial charges, q , used for the starting configuration of the *EPSR* simulation.

$r_{C-Cl} / \text{Å}$	1.758		
$r_{C-H} / \text{Å}$	1.085*		
$\gamma_{Cl-C-Cl} / ^\circ$	111.3		
$\gamma_{Cl-C-H} / ^\circ$	107.5		
$\sigma / \text{Å}$	C: 3.800	H: 0	Cl: 3.470
$\varepsilon / \text{kJ mol}^{-1}$	C: 0.3138	H: 0	Cl: 1.2552
q / e	C: -0.050	H: 0.185	Cl: -0.045

* changed from 1.1 Å to give a better fit to our data.

From a structural model of chloroform, six radially averaged pair-correlation functions can be obtained, $g_{C-C}(r)$, $g_{C-H}(r)$, $g_{C-Cl}(r)$, $g_{H-H}(r)$, $g_{H-Cl}(r)$ and $g_{Cl-Cl}(r)$. These are related to the corresponding partial structure factors, $S_{A-B}(Q)$, by Fourier sine transform⁷

$$S_{A-B}(Q) = 1 + \frac{4\pi\rho_0}{Q} \int_0^\infty r [g_{A-B}(r) - 1] \sin(Qr) dr \quad \text{Eq. S2}$$

where ρ_0 is the atomic number density. A total structure factor, $F(Q)$, can then be calculated from the weighted sums of the partial structure factors.

$$F(Q) = \sum_{A \leq B} (2 - \delta_{A-B}) w_{A-B} (S_{A-B}(Q) - 1) \quad \text{Eq. S3}$$

The Kronecker delta, δ_{A-B} , ensures that ‘like’ terms, for which $A = B$, are not counted twice. The weighting factors, w_{A-B} , by which the partial structure factors contribute to $F(Q)$ depend on the atomic fractions of the different types of atoms, c_A , and their neutron scattering lengths b_A .⁷

$$w_{A-B} = c_A c_B b_A b_B \quad \text{Eq. S4}$$

The weighting factors of the various atom pairs for CHCl₃, CDCl₃ and C(H/D)Cl₃ are given in Table S2. Due to the difference in neutron scattering length between ¹H (-3.74 fm) and D (6.67 fm) all $S_{A-B}(Q)$ s related to H, $S_{C-H}(Q)$, $S_{H-H}(Q)$ and $S_{H-Cl}(Q)$, contribute differently to the $F(Q)$ s of the three isotopically different liquids.

Table S2. Weighting factors, w_{A-B} , indicating the relative contributions of the partial structure factors, $S_{A-B}(Q)$ s, to the total structure factors, $F(Q)$ s.

	CHCl_3	C(H/D)Cl_3	CDCl_3
$w_{\text{C-C}} / \text{fm}^2$	1.77	1.77	1.77
$w_{\text{C-H}} / \text{fm}^2$	-1.99	0.78	3.55
$w_{\text{C-Cl}} / \text{fm}^2$	15.28	15.28	15.28
$w_{\text{H-H}} / \text{fm}^2$	0.56	0.09	1.78
$w_{\text{H-Cl}} / \text{fm}^2$	-8.60	3.38	15.33
$w_{\text{Cl-Cl}} / \text{fm}^2$	33.02	33.02	33.02

In principle, to fully describe the structure of liquid chloroform all six $S_{A-B}(Q)$ s need to be known. However, since only three $F(Q)$ s with different hydrogen contrasts are available from our experiment, *EPSR* is required to estimate some of the missing structural information. To prepare the final structural model *EPSR* compares simulated $F(Q)$ data with the experimental $F(Q)$ s and introduces so-called empirical potentials between the atom pairs in the structural model in an iterative process until the simulated $F(Q)$ s provide the best possible fit to the experimental $F(Q)$ s. The best fits obtained for the 25 and -53°C datasets are shown in Figure 1 and Figure S1, respectively. Figure S2 shows the intermolecular parts of the six $g_{A-B}(r)$ functions of the best fit *EPSR* models for chloroform at 25 and -53°C .

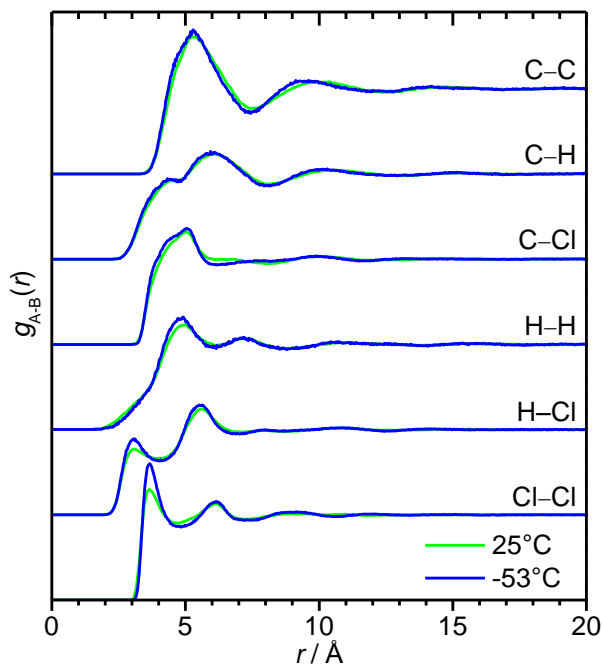


Figure S2. Intermolecular parts of the $g_{A-B}(r)$ pair-correlation functions of liquid chloroform at 25°C (green) and -53°C (blue).

The quality of the fits to the experiment data can be quantified by calculating the sums of the absolute differences between the simulated and experimental data over all three samples. For the room temperature

data and the Q -range shown in Fig. 1 these sums take values of $4.14 \text{ b sr}^{-1} \text{ atom}^{-1}$ for the starting structure and $3.13 \text{ b sr}^{-1} \text{ atom}^{-1}$ after the best fits have been obtained using the empirical potentials. The most pronounced improvements to the fits were observed in the 1 to 4 \AA^{-1} Q -range which is primarily sensitive to intermolecular correlations. In summary, it can be concluded that the potential parameters from ref. 6 produce a very reasonable starting structure. Yet, the additional descriptive power of the empirical potentials is needed in order to obtain the best possible fits to the experimental data.

4 Structural analysis

The various angle-dependent correlation functions shown in Figure 2 and 3 were obtained by fitting generalized spherical harmonic functions^{8, 9} to the partial structure factors using the *EPSR* auxiliary routines *SHARM* or *SDF*. The spherical harmonic functions made use of the following Clebsch-Gordon coefficients: $l = 0, 1, 2, 3, 4$; $l_1 = 0, 1, 2, 3, 4$; $l_2 = 0, 1, 2, 3, 4$; $n_1 = 0, 1, 2, 3, 4$; $n_2 = 0, 1, 2, 3, 4$. The input parameters used to create the plots in Figures 2 and 3 with the *plot2D* or *plot3D* programmes are listed in Table S3.

Table S3. Input parameters for the plotting programmes to visualize the angle-dependent correlation functions.

	$g(r, \theta)$	$g(r, \theta, \phi)$	$g(r, \alpha)$
Figure	2b,d	2c,e	3a
plotting programme	<i>plot2d</i>	<i>plot3d</i>	<i>plot2d</i>
l_1	1, 2, 3, 4	1, 2, 3, 4	1, 2, 3, 4
l_2	0	0	1, 2, 3, 4
n_1	0	1, 2, 3, 4	0
n_2	0	0	0
m	0	0	1

5 Comparison with X-ray diffraction data

X-ray diffraction relies on the scattering of X-ray radiation by the electrons of the atoms present in a sample.⁷ For this reason, the way in which the various partial structural factors contribute to the X-ray total structure factor is different compared to neutron diffraction. In the case of chloroform, the partial structure factors related to Cl contribute the most and the ones related to H the least to the X-ray total structure factor. A Panalytical X'pert Pro diffractometer equipped with a silver-anode X-ray tube ($K_\alpha = 0.56 \text{ \AA}$) and a focusing mirror was used to collect total scattering X-ray diffraction data of chloroform at 25°C in a borosilicate capillary. The data was reduced using the *GudrunX* software package. Figure S3 shows that the X-ray total structure factor of chloroform is consistent with the *EPSR*-derived structural model from neutron data which provides an additional independent test of our structural model.

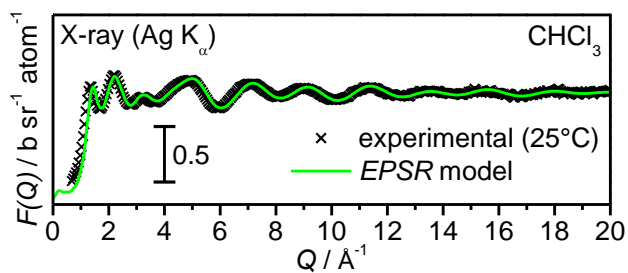


Figure S3. Experimental (black crosses) and *EPSR*-derived X-ray total structure factor (green) for liquid chloroform at 25°C.

6 Kirkwood correlation factor from dielectric spectroscopy and the *EPSR*-derived model

The Kirkwood correlation factor, g_K , indicates the net relative dipole alignment of polar molecules in liquids^{10, 11} and is defined as

$$g_K = 1 + N \langle \cos \alpha \rangle \quad \text{Eq. S5}$$

where N is the number of contributing molecular dipoles and $\langle \cos \alpha \rangle$ the average of the cosines of the relative dipole alignments. For liquids with tendencies for parallel dipole alignment g_K is greater than one. Values smaller than one indicate that antiparallel dipole alignments are favoured.

Using the Kirkwood-Fröhlich equation (eq. S6),^{12, 13} g_K can be estimated for chloroform as 1.26 at 298 K from the static dielectric constant ϵ (4.80),¹⁴ the high-frequency dielectric constant ϵ_∞ (2.17),¹⁵ the vapour-phase dipole moment μ_0 (1.04 D)¹⁴ and the number density of molecules ρ (0.0748 Å⁻³). Sigvartsen *et al.*, have estimated a value 1.40 for g_K using slightly different values for the various physical quantities.¹⁶

$$g_K = \frac{(\epsilon - \epsilon_\infty)(2\epsilon + \epsilon_\infty)}{\epsilon(\epsilon_\infty + 2)^2} \cdot \frac{9kT}{4\pi\rho\mu_0^2} \quad \text{Eq. S6}$$

In addition to estimating g_K from dielectric data it can also be calculated from the *EPSR*-derived structural model using the $h_{\text{COM-COM}}(l=1, l_1=1, l_2=0; n_1=0, n_2=0; r)$ function which contains the relative dipole alignment information and is obtained from spherical-harmonic expansion (*cf.* chapter 4).¹⁷

$$g_K(r_{\text{max}}) = 1 - \frac{1}{3\sqrt{3}} \rho \int_0^{r_{\text{max}}} 4\pi r^2 h_{\text{COM-COM}}(110; 00; r) dr \quad \text{Eq. S7}$$

The distance-dependent Kirkwood correlation function, $g_K(r_{\text{max}})$, is shown in Figure S4 which tends towards g_K with increasing r_{max} . Using r_{max} of 20 Å, the g_K value of the *EPSR*-derived model structure of liquid chloroform can be estimated as 1.56 ± 0.35 which is, within the margins of error, in agreement with the values obtained from dielectric spectroscopy.

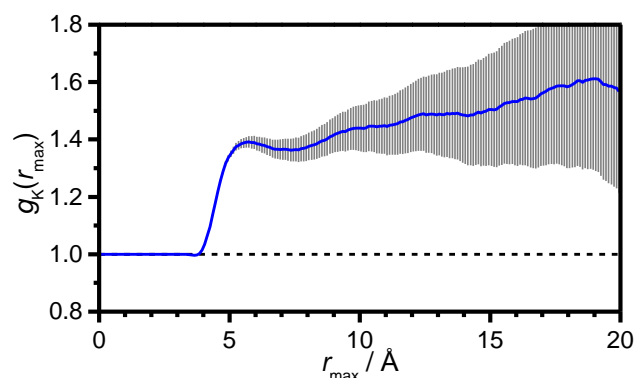


Figure S4. The distance-dependent Kirkwood correlation function derived from the *EPSR* structural model.

The limitations in obtaining more accurate g_K values from structural models are that the integration is only possible to finite values of r_{\max} and the increasing contributions of noise at larger distances. However, the values derived from dielectric data are also affected by systematic errors due to simplifications made in the derivation of the Kirkwood-Fröhlich equation.¹² Furthermore, ϵ_∞ is typically difficult to measure and therefore often only estimated from an empirical relationship with the refractive index.¹⁸

In summary, both dielectric spectroscopy and our diffraction study show a tendency for parallel dipole alignment in chloroform. We emphasise that while dielectric spectroscopy gives highly accurate information on the bulk dielectric properties of polar liquids, diffraction studies offer the great advantage in that they provide direct insights into their local structures.

7 References

1. A. K. Soper, *Molecular Physics*, 2009, **107**, 1667-1684.
2. A. K. Soper, *Chem. Phys.*, 1996, **202**, 295-306.
3. A. K. Soper, *Phys. Rev. B*, 2005, **72**, 104204.
4. D. R. Lide and H. V. Kehiaian, *CRC Handbook of Thermophysical and Thermochemical Data*, CRC Press, Boca Raton, USA, 1994.
5. M. Jen and D. R. Lide, *J. Chem. Phys.*, 1962, **36**, 2525-2526.
6. V. E. Barlette, F. L. L. Garbujo and L. C. G. Freitas, *Mol. Eng.*, 1997, **7**, 439-455.
7. D. S. Sivia, *Elementary Scattering Theory*, Oxford University Press, Oxford, 2011.
8. C. G. Gray and K. E. Gubbins, *Theory of Molecular Fluids, Volume 1: Fundamentals*, Clarendon Press, Oxford, 1984.
9. A. K. Soper, in *Local Structure from Diffraction*, eds. S. J. Billinge and M. F. Thorpe, Plenum Press, New York, 1998.
10. J. G. Kirkwood, *J. Chem. Phys.*, 1939, **7**, 911-919.
11. N. Deba, A. S. Tiwaryb and A. K. Mukherjee, *Mol. Phys.*, 2010, **108**, 1907-1917.
12. H. Fröhlich, *Trans. Faraday Soc.*, 1948, **44**, 238-243.
13. P. H. Fries, *Mol. Phys.*, 1997, **90**, 841-853.
14. R. Lide, ed., *CRC Handbook of Chemistry and Physics*, 77th edn., CRC press, Boca Raton, 1996.

15. L. C. Rosenthal and H. L. Strauss, *J. Chem. Phys.*, 1976, **64**, 282.
16. T. Sigvartsen, B. Gestblom, E. Noreland and J. Songstad, *Acta Chem. Scand.*, 1989, **43**, 103.
17. A. K. Soper, *J. Chem. Phys.*, 1994, **101**, 6888-6901.
18. L. Simeral and R. L. Amey, *J. Phys. Chem.*, 1970, **74**, 1443-1446.